

Prospects for Detecting Oxygen, Water, and Chlorophyll in an Exo-Earth

Timothy D. Brandt* and David S. Spiegel*

*School of Natural Sciences, Institute for Advanced Study, Princeton, NJ, USA.

Submitted to the Proceedings of the National Academy of Sciences of the United States of America on March 26, 2022.

The goal of finding and characterizing nearby Earth-like planets is driving many NASA high-contrast flagship mission concepts, the latest of which is known as the Advanced Technology Large-Aperture Space Telescope (ATLAST). In this article, we calculate the optimal spectral resolution $R = \lambda/\delta\lambda$ and minimum signal-to-noise ratio per spectral bin (SNR), two central design requirements for a high-contrast space mission, in order to detect signatures of water, oxygen, and chlorophyll on an Earth twin. We first develop a minimally parametric model and demonstrate its ability to fit model Earth spectra; this allows us to measure the statistical evidence for each component's presence. We find that water is the most straightforward to detect, requiring a resolving power $R \gtrsim 20$, while the optimal resolving power for oxygen is likely to be closer to $R = 150$, somewhat higher than the canonical value in the literature. At these resolutions, detecting oxygen will require ~ 3 times the SNR as water. Chlorophyll, should it also be used by alien plants in photosynthesis, requires ~ 6 times the SNR as oxygen for an Earth twin, only falling to oxygen-like levels of detectability for a very low cloud cover and/or a very large vegetation covering fraction. This suggests designing a mission for sensitivity to oxygen and adopting a multi-tiered observing strategy, first targeting water, then oxygen on the more favorable planets, and finally chlorophyll on only the most promising worlds.

Exoplanets | Atmospheres | Astrobiology | Biosignatures

Significance

One of NASA's most important long-term goals is to detect and characterize terrestrial exoplanets, and to search their spectra for signs of alien life. This overarching goal is currently driving concepts for a future high-contrast flagship mission. We determine the fidelity with which such a mission would need to measure an exo-Earth's spectrum in order to detect oxygen, water, and chlorophyll. Our results suggest that a well-designed space mission could detect O₂ and H₂O in a nearby Earth twin, but that it would need to be significantly more sensitive (or very lucky) to see alien chlorophyll. We suggest designing the instrument with an eye towards oxygen, and perhaps looking for chlorophyll around one or a few exceptional targets.

Introduction

While indirect methods have now discovered several thousand exoplanets (1, 2, 3), most of these are currently inaccessible to characterization. Direct imaging offers the ability to observe an exoplanet in either thermal or reflected light, and provides a window on the structure and composition of its atmosphere. Ultimately, one of NASA's goals is to find and characterize terrestrial exoplanets around nearby stars and to search for molecules and biosignatures. The *Terrestrial Planet Finder* (TPF, e.g. 4, 5) was one mission concept with this goal in mind, while the *Advanced Technology Large-Aperture Telescope* (ATLAST, 6) represents a more recent proposal. Such a mission would target at least the optical wavelength range from ~ 0.5 to ~ 1 μm in order to look for spectral indications of molecular oxygen (O₂), ozone (O₃), and water (H₂O). These molecules are the most prominent absorbers in this spectral range, and are all critical species for terrestrial life. From ~ 1 to 4 μm , Earth's spectrum is dominated by a series of very strong water features, with broad overlapping CO₂ and CH₄ bands (7).

Several studies have looked at the prospects for detecting biosignatures on an Earth twin (8, 9, 10), or for learning about an exo-Earth's surface from phase variations in its colors (11, 12, 13, 14). Unfortunately, features that are biosignatures in Earth's spectrum, may not necessarily be so in a terrestrial exoplanet. The composition of Earth's atmosphere, including its oxygen abundance, has changed enormously throughout life's existence (15), while diatomic oxygen can, under some circumstances, also be produced abiotically (16). More speculatively, chlorophyll shows a strong increase in its albedo around 0.7 μm (the "red edge"), which could be detected on an exo-Earth (17, 18). Such an argument relies on the uniqueness of the chlorophyll family of molecules as the basis for photosynthesis (19).

In this paper, we consider only the detectability of surface and atmospheric constituents, neglecting their biological implications. We make as few assumptions as possible about the (highly uncertain) performance of a future high-contrast space mission. Rather than working from an instrument to detectability, we turn the problem around, and attempt to quantify the optimal design and minimum performance needed to reach NASA's terrestrial planet characterization goals.

Terrestrial Planet Spectra

We begin with a rough, but approximately correct, model of a terrestrial planet spectrum in reflection. We assume a (wavelength-dependent) surface albedo α_λ , a cloud albedo c_λ , a cloud fraction f_c , an optical depth to Rayleigh scattering \mathcal{R}_λ (assumed to be small), and absorption profiles for the most important species in Earth's atmosphere. We write the latter profiles as wavelength-dependent optical depths for each species given Earth's atmosphere's composition and pressure. Defining the full atmosphere's optical depth to absorption (for a photon traveling through the atmosphere twice) as

$$\tau_\lambda = \sum_{\text{mol}} \tau_{\lambda, \text{mol}}, \quad [1]$$

where the sum is over molecular species (O₂, O₃, and H₂O in the optical), our full model becomes

$$\frac{F_{\text{refl}}}{F_\star} \approx \frac{\mathcal{R}_\lambda}{2} f_c e^{-\tau/4} + \left(1 - \frac{\mathcal{R}_\lambda}{2}\right) f_c c_\lambda e^{-\tau/2} + \mathcal{R}_\lambda (1 - f_c) e^{-\tau/2} + (1 - \mathcal{R}_\lambda) (1 - f_c) \alpha_\lambda e^{-\tau}, \quad [2]$$

where F_\star is the incident (stellar) flux on the planetary atmosphere, and F_{refl} is the reflected flux. The first term approximates Rayleigh scattering above the clouds, the second term accounts for scattering by the clouds themselves, the third term is Rayleigh scattering above the surface, and the last term is scattering by the surface (we have dropped all terms with \mathcal{R}^2). All Rayleigh scattering is approximated

Reserved for Publication Footnotes

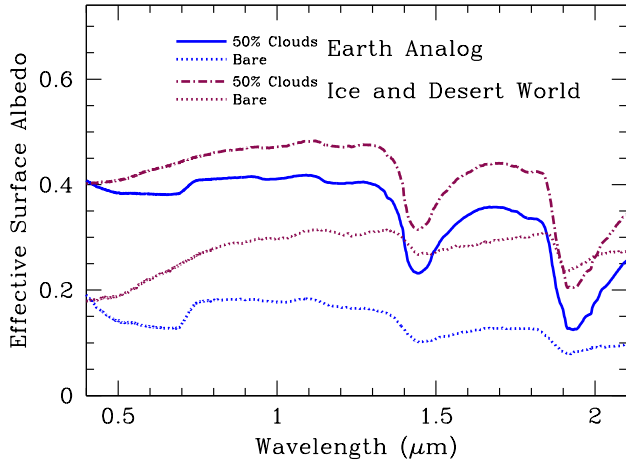


Fig. 1. Effective surface albedos, including clouds but neglecting atmospheric scattering and absorption, for two hypothetical terrestrial planets. The Earth twin is 70% water, 10% lush vegetation, 10% sand, 5% snow, and 5% dry grass by surface area, while the desert world is 30% water, 60% sand, and 10% snow. The spectral albedos for a cloudy Earth twin and a desert world are both nearly featureless across our spectral range, from ~ 0.5 to $\sim 1 \mu\text{m}$.

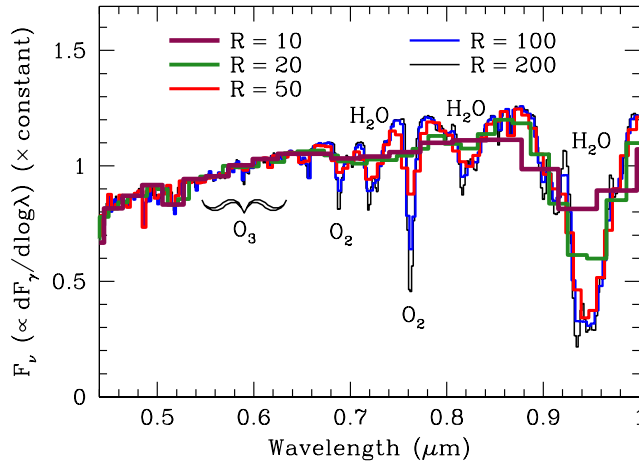


Fig. 2. Comparison of our spectrum of an Earth twin convolved to a given spectral resolution with a Gaussian line-spread function. The prominent O_2 absorption feature at $0.76 \mu\text{m}$ becomes completely blended with neighboring water features for $R \lesssim 20$, while the O_3 feature is wide and shallow, and very difficult to see.

as occurring below half the available atmosphere, and the λ subscript on τ is understood.

We use the ASTER spectral library (20) for our surface albedo measurements excepting water, an approximation based on (21) for oceans (including a substantial correction for specular reflection at blue wavelengths), (22) for water cloud albedos, and (7) for the absorption profiles of prominent atmospheric species. We take our normalization of the Rayleigh scattering optical depths for Earth’s atmosphere from (23). We take a 50% cloud coverage, noting that its main effect is simply to obscure spectral features from the surface (cloud albedos are gray to an excellent approximation, while photons must still travel through at least $\sim 1/2$ the atmosphere). The effective albedo of clouds is ~ 60 – 65% across the wavelength range, washing out surface spectral features by a factor $\gg 1$ when the clouds are optically thick.

Figure 1 shows the spectral surface albedos, including clouds and surface materials but neglecting the atmosphere, for two hypothetical terrestrial planets. One is Earth-like, with 70% water, 10% lush vegetation, 10% sand and bare soil (brown loamy fine sand from ASTER), 5% snow, and 5% dry grass, consistent with the estimates based on data from the MODerate resolution Imaging Spectroradiometer (MODIS, 24) and tabulated in (11). The second is a “desert world,” with a basic character similar to Earth, but lacking vegetation and with a somewhat lower water coverage. We assume this world to have 30% water, 60% sand, and 10% snow by area. Within the spectral region we are targeting, from $\sim 0.5 \mu\text{m}$ to $\sim 1 \mu\text{m}$, the spectral albedos of both a cloudy Earth twin and a desert world are nearly featureless. This is not true in the near-infrared. While we focus on the cloudy Earth twin for the rest of this paper, our results would be almost identical for the desert world.

We create mock spectra from our models by smoothing the output of Equation [2] to an adopted spectral resolution using a Gaussian line-spread function,

$$f(\delta \log \lambda) \propto \exp\left(-\frac{1}{2}(\delta \ln \lambda)^2 \left(R\sqrt{8 \ln 2}\right)^2\right), \quad [3]$$

where R is the (dimensionless) characteristic spectral resolution $\lambda/\delta\lambda$, the full width at half maximum of the Gaussian. We assume that these spectra are sampled at a rate $\lambda/\delta\lambda = R\sqrt{8 \ln 2} \approx 2.35R$, the inverse standard deviation of the Gaussian, and roughly the critical sampling rate. Binning the spectra, in contrast, would be equivalent to convolving with a boxcar line-spread function and sampling at half the critical rate. Such undersampling makes spectral reconstruction dependent on excellent knowledge of the line-spread function and even on the centers chosen (often arbitrarily) for the wavelength bins. Finally, we convert our units into flux density f_ν , proportional to photons per logarithmic wavelength bin. The resulting flux density is approximately constant (within a factor of ~ 1.5) across our wavelength range. We further assume that noise, whether from speckle residuals, background photon noise, read noise, or some other source, is also a constant across the wavelength range, so that the signal-to-noise ratio per λ/R bin (SNR) is nearly independent of wavelength (apart from the centers of spectral lines, where the signal drops). Note that, with our sampling and definitions, the SNR per resolved bin is $(8 \ln 2)^{1/4} \approx 1.53$ the SNR per sample.

Figure 2 shows approximate noiseless spectra of an Earth twin at full phase for a variety of spectral resolutions. For spectral resolutions $R \lesssim 20$, the prominent $0.76 \mu\text{m}$ O_2 absorption feature becomes almost completely blended with neighboring water features, making the spectrum flat. The ozone band centered at $\lambda \sim 0.59 \mu\text{m}$ is both broad and shallow, making it difficult to see at any spectral resolution. Water features, on the other hand, remain conspicuous down to $R \sim 20$.

A Minimally Parametric Model

We assume as a baseline that the spectrum of a hypothetical terrestrial exoplanet will be modeled using a combination of a known stellar spectrum, absorption spectra of possible atmospheric constituents, and Rayleigh scattering. Unfortunately, a space mission capable of achieving contrasts of 10^{10} will be unlikely to have perfect spectrophotometric calibration of a faint exoplanet. Surface materials have spectral albedos that vary across the visible wavelength range, though most plausible surface materials, including soils, snow, and water, lack sharp spectral features from ~ 0.5 to $1 \mu\text{m}$. We therefore assume as our baseline that a future analysis will not attempt to fit the surface composition, which will, in any case, be at least somewhat degenerate with the optical depth to Rayleigh scattering and with uncertain spectrophotometric calibrations. Instead, we fit our

spectra with a model of the form

$$\frac{F_\lambda}{F_{\lambda,*}} \approx \left(\sum_i A_i \lambda^i \right) \left[\exp \left(- \sum_{\text{mol}} \tau_{\lambda,\text{mol}} \right) + \frac{c}{\lambda^4} \exp \left(- \sum_{\text{mol}} \frac{\tau_{\lambda,\text{mol}}}{2} \right) \right], \quad [4]$$

where $\tau_{\lambda,\text{mol}} \geq 0$ is the optical depth of a given molecular species and the last term, a polynomial, accounts for uncertainties in the surface (and cloud) spectral albedo and spectrophotometric calibration. We crudely include Rayleigh scattering with a term c/λ^4 , making the approximation that all Rayleigh scattering occurs beneath half the atmosphere. We caution against interpreting the Rayleigh-like term too literally; it also combines with the polynomial term to add flexibility to account for the unknown surface albedo.

Equation [4] presents the challenge of fitting our mock terrestrial planet spectra as a well-posed χ^2 problem (though not a linear one), with the parameters in Equation [4] chosen to minimize

$$\chi^2 = \sum_\lambda \frac{(F_{\lambda,\text{obs}} - F_{\lambda,\text{model}})^2}{\sigma_\lambda^2}. \quad [5]$$

The model as we apply it to our mock data has up to seven free parameters: a column density for each of three molecular species (O_2 , O_3 , and H_2O), a normalization of Rayleigh scattering, and three coefficients for a quadratic polynomial normalization. It allows us to calculate the likelihood of the best-fit model with and without a given chemical species, with the likelihood ratio giving the confidence with which that species can be said to be present in the atmosphere. This likelihood ratio may be considered a figure of merit for a future high-contrast space mission, and will certainly be a function of its spectral resolution.

Finally, in addition to the atmospheric species O_2 , O_3 , and H_2O that dominate optical absorption in Earth's atmosphere, we extend our model by adding one additional template for the red edge of chlorophyll absorption. We use a softened Heaviside function

$$H(\lambda) = [1 + \exp(80(0.72 - \lambda/\mu\text{m}))]^{-1}, \quad [6]$$

with the center and width chosen to match the feature in vegetation in the ASTER libraries. Equation [4] becomes

$$\frac{F_\lambda}{F_{\lambda,*}} \approx \left(\sum_i A_i \lambda^i \right) \left[(1 + bH(\lambda)) \exp \left(- \sum_{\text{mol}} \tau_{\lambda,\text{mol}} \right) + \frac{c}{\lambda^4} \exp \left(- \sum_{\text{mol}} \frac{\tau_{\lambda,\text{mol}}}{2} \right) \right]. \quad [7]$$

This requires one additional free parameter to look for chlorophyll, or two free parameters to look for a molecule with a similar absorption edge but at unknown wavelength.

Figure 3 shows the results of our fitting (without the extra parameter(s) for chlorophyll) for an ambitious space mission ($R = 150$, $\text{SNR} = 8$, for a SNR per sampling of 5.2) suitable for finding atmospheric O_2 . The top panel shows the true input spectrum (blue, Equation [2]), the input spectrum with one realization of Gaussian noise (black), and our recovered spectrum (red). The quality of the fit is excellent. In the limit of many realizations of Gaussian noise, the mean χ^2 of the fit is within 1.5 of the number of degrees of freedom, much less than 24, the root variance of the χ^2 distribution for 293 degrees of freedom. In other words, our simple model (which declines to fit the spectral albedo in any detail) provides a perfectly satisfactory fit even for this high-SNR case.

The bottom panel of Figure 3 shows the best-fit spectrum from the top panel decomposed by the individual terms in Equation [4]. We have smoothed the spectra to $R = 1000$ for illustration purposes.

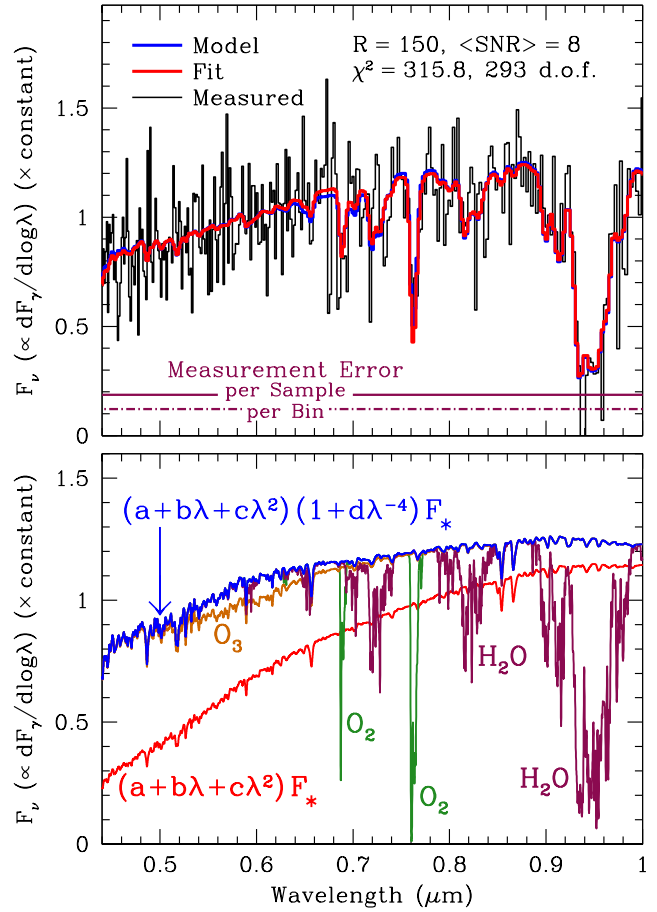


Fig. 3. Results of fitting Equation [4] to a realization of a high SNR spectrum of an Earth twin ($R = 150$, $\text{SNR} = 8$ per bin, 5.2 per sample). Top panel: the true input spectrum (blue, Equation [2]), the spectrum with one realization of Gaussian noise (black), and the recovered model spectrum (red). The quality of the fit is excellent; indeed, for many realizations, the mean χ^2 is within 1.5 of the number of degrees of freedom. Bottom panel: the best-fit spectrum from Equation [4] (the red curve in the top panel) decomposed by terms, at $R = 1000$. We caution against interpreting the “Rayleigh” term ($\propto \lambda^{-4}$) too literally, as this term ends up including much of the spectral variation in albedo.

The polynomial fit (red curve) is redder than the Solar spectrum, while including the “Rayleigh term” gives a spectrum bluer than Solar. Interpreting this “Rayleigh term” naively would lead to an overestimate by a factor of a few of the optical depth of Earth's atmosphere. In practice, the term is strongly covariant with the free polynomial; the terms combine to fit broad spectral variations in cloud and surface albedos (which are not negligible, as Figure 1 shows). What this exercise *does* show is that we may safely neglect the spectral albedos, treating them as nuisance parameters, when looking for the spectral signatures of molecules.

False Positives and Significance Thresholds

In the previous section, we showed that our model offers an acceptable fit to the spectrum of an Earth analog even for a high-SNR observation with $R = 150$ and $\text{SNR} = 8$. We now seek to quantify the significance of a possible detection of water, oxygen and/or ozone in the exoplanet's atmosphere. In order to do this, we return to the formalism of χ^2 , and use the improvement in the χ^2 parameter with the addition of a molecular absorption template (as a free parameter) to

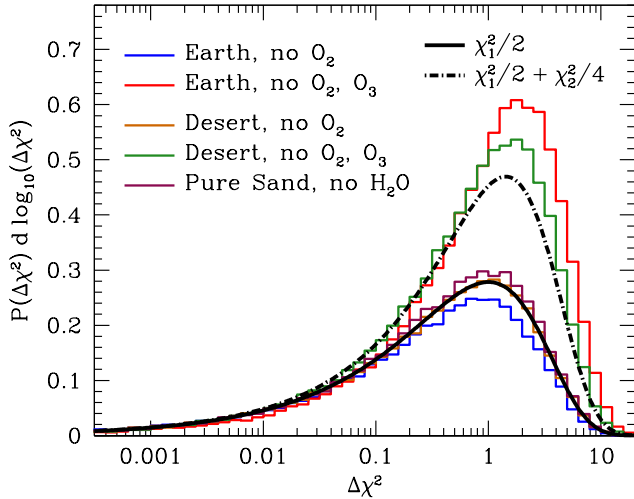


Fig. 4. Distributions of the improvements in χ^2 by adding an additional degree of freedom represented by a species *not* present in a model atmosphere. The O_2 and H_2O fits are consistent with the relevant χ^2 distributions after accounting for the fact that we constrain all optical depths to be positive; the O_2+O_3 fits disagree somewhat in the tails. We use the χ^2 distributions to set $\Delta\chi^2$ thresholds for a given false-alarm probability.

measure the evidence for that species' presence. We first show that the improvement in χ^2 is given by the appropriate χ^2 distribution in the case where the molecular species is *not* present. To perform this test, we create a series of mock atmospheres omitting the appropriate absorption templates (equivalently, setting their optical depths to zero). We then fit for the parameters in Equation [4] either fixing the $\tau_{mol} = 0$ or allowing them to remain free. This allows us to compute the probability of a false positive, set an appropriate detection threshold, and measure the probability of detection in an atmosphere that does contain the molecule.

Figure 4 shows the results of this test for our Earth analog with 50% cloud cover, first neglecting O_2 and then neglecting both O_2 and O_3 . We perform the same test on our desert world assuming a 30% cloud cover, and finally on a dry exoplanet with a surface composed of 100% sand and rock. In the cases of O_2 and H_2O , the addition of an (unwarranted) extra degree of freedom produces a distribution of improvement in χ^2 values that matches the theoretically expected curve extremely well, even in the tails. The theoretical curves for a single parameter are divided by 2 because the positivity constraint on each optical depth forbids half of their best-fit values in the case of symmetric Gaussian noise: half of the distribution is a delta function at zero. The distribution in the case of two missing atmospheric components, O_2 and O_3 , is not quite a linear combination of χ_1^2 and χ_2^2 , the χ^2 distributions with one and two degrees of freedom, particularly in the tails. Ozone's $\sim 0.6 \mu\text{m}$ band is a broad and shallow spectral feature that can combine with the Rayleigh term and poly-

nomial term in Equation [4] to reproduce a wider range of surface spectral albedos.

Figure 4 demonstrates that we can establish our false positive thresholds using the appropriate χ^2 distributions, at least in the case of O_2 and H_2O . In these cases, with a single molecular species, a threshold $\Delta\chi^2 = 9.6$ gives a false positive probability of 10^{-3} , while $\Delta\chi^2 = 13.8$ gives a false positive probability of 10^{-4} . With two molecular species, the thresholds for a 10^{-3} and 10^{-4} false positive rate would become 11.8 and 16.3, respectively, if they were described by the χ^2 distributions shown. Our analysis actually shows that the thresholds should be closer to $\Delta\chi^2$ of 14 and 19 for 10^{-3} and 10^{-4} false-alarm probabilities, respectively, in the Earth twin. For the desert world, with its simpler spectral albedo, the thresholds become roughly 12.4 and 17.5. Crucially, and unlike in the case of O_2 and H_2O , these significance thresholds depend on the planet's spectral albedo.

Detecting Components of the Atmosphere and Surface

We now turn to the probability of detecting an atmospheric constituent given our model spectra, our seven-parameter fitting routine, and an adopted false positive threshold (which we take to be either 10^{-3} or 10^{-4}). In addition to the species being targeted, these detection probabilities depend on the spectral resolution and noise level, so that the probability for each species resides in a two-dimensional space.

For consider three paths through the space of resolution and noise level. In a best-case scenario, the intrinsic spectral resolution is arbitrarily high, so that the spectra may be binned to any resolution of interest with no additional noise. This corresponds to the ideal background-limited case. The variance per bin then scales as R^{-1} , and SNR as $R^{-1/2}$. We consider the worst-case scenario to be that for which the variance per bin is independent of bin size. This would hold, for example, in a read-noise-limited instrument which simply varied the dispersion, holding everything else fixed. The SNR in this case would scale as R^{-1} . Finally, we consider an intermediate case in which SNR scales as $R^{-3/4}$. We normalize all of these paths at $R = 50$. Table 1 summarizes our results, which we discuss in detail in the following sections.

Oxygen and Ozone. The left panel of Fig. 5 shows our results for the case of atmospheric O_2 . Given a SNR of 10 at $R = 50$, the optimal resolution for an O_2 detection varies from ~ 150 to many hundreds, with a value of $R \sim 300$ for our intermediate noise case. At $R = 300$, we would need SNR $\gtrsim 4$ for a likely detection; this corresponds to SNR ≈ 10 at $R = 50$ in our best-case noise scaling.

Ultraviolet photons from the star will convert diatomic oxygen into ozone, so we may also ask if it would be easier to detect atmospheric oxygen in our model by simultaneously searching for both O_2 and O_3 . In the case of an Earth twin, the answer is no: the extra degree of freedom increases the $\Delta\chi^2$ threshold, and the depth of the ozone feature is insufficient to compensate (see Figure 3). The ozone feature is also broad ($\Delta\lambda/\lambda \sim 0.1$) and occurs just redward of a major upturn in albedo from Rayleigh scattering, making it somewhat degenerate with spectrophotometric uncertainties. This is reflected in significance thresholds somewhat higher than for the relevant χ^2 distributions (as shown in Figure 4).

While fitting for both O_2 and O_3 does not improve the detection probabilities for an Earth twin, it could help for a terrestrial planet with a significantly higher ozone column. This could arise either from a higher UV flux (from an F-star, for example), from a significantly lower concentration of molecules and ions to catalyze ozone's decomposition, or both. However, as noted earlier, any analysis simultaneously searching for O_2 and O_3 would need to higher significance threshold to account for ozone's ability to mimic a variable spectral albedo.

Table 1. Approximate Optimal Resolutions and Minimum SNRs

Species	\tilde{R}	$\text{SNR}_{\tilde{R}}^*$	SNR_{150}^*
H_2O	40	5	2.3
O_2	150	6	6
Chlorophyll	20	120	40

*90% detection probability for 10^{-3} false positive rate

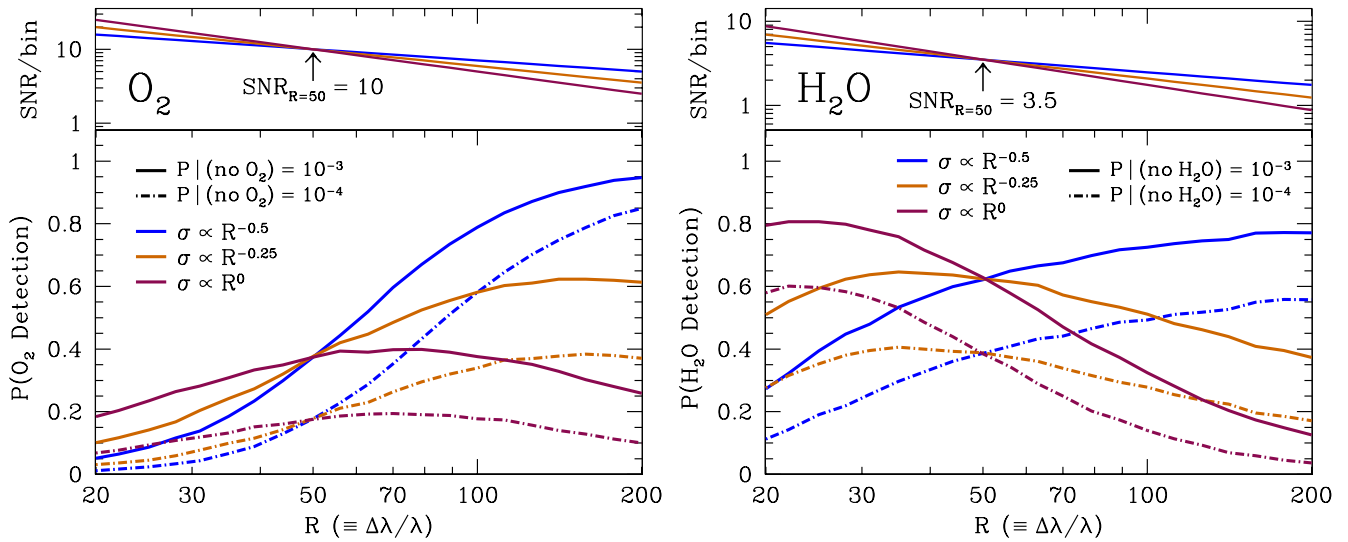


Fig. 5. Probability of detecting of O₂ (left) and H₂O (right) on an Earth twin as a function of spectral resolution and SNR. All curves are normalized to a common SNR at $R = 50$, $\text{SNR} = 10$ for O₂ and $\text{SNR} = 3.5$ for H₂O. The curves are scaled to either reproduce the read-noise-limited case (burgundy line) in which SNR scales as R^{-1} , the perfect background-limited case (blue line) in which SNR scales as $R^{-1/2}$, or an intermediate case (orange line). The solid lines indicate a false-alarm probability of 10^{-3} , while the dot-dashed lines have a false-alarm probability of 10^{-4} . *Left:* The optimal resolution in the intermediate case is $R \sim 150$, with a corresponding minimum SNR of ~ 5 . *Right:* The optimal resolution in the intermediate case is $R \sim 40$, where the minimum SNR is ~ 5 . This is a factor of ~ 2 – 3 lower than the scaled SNR needed to detect O₂ in the same Earth twin.

Water. Water has a series of deep absorption features from the red end of the visible into the near-infrared, with a variety of effective widths, making it easier to detect than diatomic oxygen. As Figure 2 suggests, water absorption remains conspicuous in the spectrum down to spectral resolutions of $R \sim 20$. At still lower resolutions, water absorption becomes more difficult to separate from variations in the surface albedo or errors in the spectrophotometric calibration.

The right panel of Fig. 5 shows the probability of a high-significance H₂O detection for an Earth twin, with all of the same assumptions used in the O₂ panel (left panel of same figure), but just over 1/3 of the fiducial SNR. For the case intermediate between the optimal and pessimal noise scalings, the optimal spectral resolution for H₂O detection is $R \sim 40$. This is a factor of several lower than for O₂ and reflects the broader widths of the features.

The Red Edge of Chlorophyll. Chlorophyll on Earth has a sharp rise in reflectivity around $0.7 \mu\text{m}$, the “red edge.” An analogous feature could be detectable on an exo-Earth, with the (large) caveat that photosynthetic aliens may use a different family of pigment molecules than their terrestrial analogs, and the understanding that any claimed detection would be extremely controversial.

We approximate the albedo of vegetation as a softened Heaviside step function (Equation [7], which provides a reasonable match in the wavelength range from ~ 0.5 to $1 \mu\text{m}$. Though the jump is very strong in pure vegetation, with the albedo increasing from $\sim 5\%$ to $\sim 50\%$, it is much weaker in an integrated Earth spectrum. This is due both to the small fraction of surface area covered by vegetation ($\sim 10\%$), and to the fact that much of this area is covered by optically thick clouds. We optimistically use the same $\Delta\chi^2$ thresholds as for O₂ and H₂O to indicate a detection. In the case of a very high SNR, the assumption that our model works well enough without modeling the cloud and surface albedos begins to break down.

The “red edge” of vegetation does not require a high spectral resolution to identify; assuming our intermediate noise scaling, a value $R \sim 20$ is optimal. Chlorophyll is, however, exceedingly difficult to detect with significance in an Earth twin. To facilitate a comparison with O₂, we explore chlorophyll’s detectability as a function of SNR,

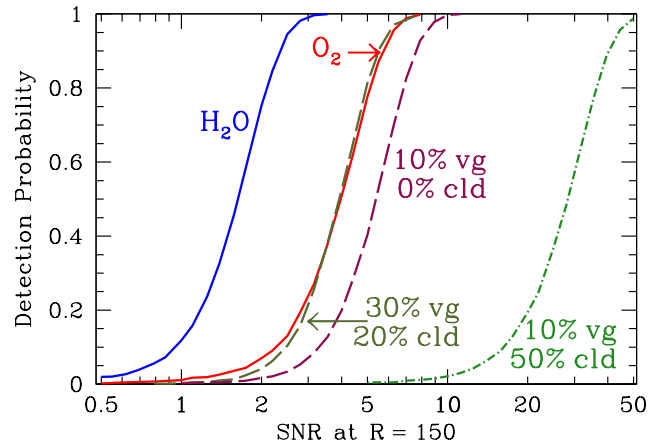


Fig. 6. Detectability of H₂O, O₂, and the red edge of chlorophyll for three terrestrial planets, assuming $R = 150$ (i.e. a mission optimized to detect O₂) and a false alarm probability of 10^{-3} . For an Earth twin, with 50% cloud coverage and 10% vegetation coverage, chlorophyll requires ~ 6 times as much SNR as O₂. Only under optimistic assumptions about cloud and vegetation cover (and the universality of chlorophyll) does the molecular family approach O₂ in detectability.

the vegetation covering fraction, and the cloud fraction, at a fiducial R of 150 (assuming a mission optimized to detect O₂).

Figure 6 shows our results. For an Earth twin, O₂ requires 2–3 times the SNR as H₂O, while chlorophyll, even if the pigment is known, requires a SNR ~ 6 times higher than O₂. At these levels, our assumption that the spectrum can be modeled with a total disregard for the details of the surface albedo begins to break down. In order for chlorophyll to become as easy to detect as oxygen, we must either assume a vegetation covering fraction of at least 30% with a light cloud cover, or a cloud-free Earth. The former scenario would have roughly half of Earth’s cloud coverage and would see all land

covered in lush greenery. The cloud-free Earth twin has a lower mean albedo, making it roughly twice as hard to achieve a given SNR. It is also difficult to imagine chlorophyll, part of a photosynthetic cycle based on water, occurring on a cloud-free world.

While a future mission will undoubtedly search for chlorophyll on nearby terrestrial planets, we argue that a high-contrast mission should be designed to achieve the easier and better-defined goals of oxygen and water detection. A plausible observing strategy would attempt to achieve the requisite SNR for O₂ and H₂O around nearby stars, and then spend an enormous amount of time attempting to reach the SNR needed to detect chlorophyll around the very best target(s).

Conclusions

In this paper we have constructed a minimally parametric model to recover the components of a terrestrial planet's atmosphere as observed by a future high-contrast space mission. We find that we can reproduce the spectrum of an Earth twin to a very high accuracy even when completely neglecting the surface albedo, apart from an overall multiplicative term quadratic in wavelength. Such a term also includes uncertainties in the spectrophotometric calibration, which are likely to be significant.

We have focused our analysis on the optical and very near-infrared spectrum. A Solar-type star is brightest at these wavelengths, giving the maximum photon flux. Diatomic oxygen and water have very prominent absorption features from ~ 0.6 to $1 \mu\text{m}$, while likely surface materials like rock, sand, and water have nearly featureless spectral albedos. By targeting shorter wavelengths, we also have the advantage of a finer diffraction-limited resolution.

We find that a future space mission will be likely to detect water on an Earth twin with a spectral resolution of $R \gtrsim 40$ and a SNR per bin of $\gtrsim 5$. Such a mission will have a much more difficult time detecting atmospheric oxygen, and is unlikely to improve its sensitivity by searching for O₂ and O₃ simultaneously, at least at visible wavelengths (ozone has a strong absorption edge at in the near-ultraviolet, at $\sim 0.3 \mu\text{m}$). For a mission targeting only O₂, we find an optimal resolution of $R \sim 150$ for our intermediate noise scaling case, and a minimum SNR of ~ 6 at $R = 150$. This is ~ 3 times the resolution of an instrument optimized to see water, and a factor of ~ 2 - 3 more challenging than water as measured by the scaled SNR.

Finally, we show that the "red edge" of chlorophyll absorption at $\lambda \sim 0.7 \mu\text{m}$ will be extremely difficult to detect, unless the cloud cover is much lower and/or the vegetation fraction is much higher than on Earth. Assuming extraterrestrial chlorophyll to have the same optical properties as the terrestrial pigments, and assuming Earth-like cloud and vegetation coverings, detecting chlorophyll will require a SNR ~ 6 times higher than for diatomic oxygen, equivalent to a $SNR \gtrsim 100$ at $R \sim 20$. The detectability only approaches that of O₂ if the cloud covering is zero, or if it is light and a much larger surface fraction, $\sim 30\%$, is covered in vegetation.

Based on our findings, we argue that a future mission should be designed towards the well-defined goal of sensitivity to O₂ and H₂O around the best candidate terrestrial exoplanets, perhaps even with two dispersing elements to achieve both $R \sim 40$ and $R \sim 150$. Extensive (and expensive) follow-up of the very best targets, preferably with O₂ and H₂O detections, might then be used to search for the red edge of chlorophyll.

ACKNOWLEDGMENTS. The authors acknowledge very helpful discussions with Michael McElwain and Edwin Turner. TDB gratefully acknowledges support from the Corning Glass Works Foundation through a membership at the Institute for

Advanced Study. DSS gratefully acknowledges support from the Association of Members of the Institute for Advanced Study.

References

- Schneider J, Dedieu C, Le Sidaner P, Savalle R, Zolotukhin I (2011) Defining and cataloging exoplanets: the exoplanet.eu database. *A&A*532:A79.
- Wright JT, et al. (2011) The Exoplanet Orbit Database. *PASP*123:412–422.
- Rein H (2012) A proposal for community driven and decentralized astronomical databases and the Open Exoplanet Catalogue. *ArXiv e-prints arXiv:12117121*.
- Beichman C (2003) Recommended Architectures for the Terrestrial Planet Finder. In Sembach KR, Blades JC, Illingworth GD, Kennicutt RC Jr, eds., *Hubble's Science Legacy: Future Optical/Ultraviolet Astronomy from Space*, vol. 291 of *Astronomical Society of the Pacific Conference Series*, p. 101.
- Levine M, et al. (2009) Terrestrial Planet Finder Coronagraph (TPF-C) Flight Baseline Concept. *ArXiv e-prints*.
- Postman M, et al. (2009) Advanced Technology Large-Aperture Space Telescope (ATLAST): A Technology Roadmap for the Next Decade. *ArXiv e-prints*.
- Rugheimer S, Kaltenegger L, Zsom A, Segura A, Sasselov D (2013) Spectral Fingerprints of Earth-like Planets Around FGK Stars. *Astrobiology* 13:251–269.
- Des Marais DJ, et al. (2002) Remote Sensing of Planetary Properties and Biosignatures on Extrasolar Terrestrial Planets. *Astrobiology* 2:153–181.
- Kaltenegger L, Selsis F (2007) *Biomarkers Set in Context* (Wiley). p. 79.
- Davies PCW, et al. (2009) Signatures of a Shadow Biosphere. *Astrobiology* 9:241–249.
- Fujii Y, et al. (2010) Colors of a Second Earth: Estimating the Fractional Areas of Ocean, Land, and Vegetation of Earth-like Exoplanets. *ApJ*715:866–880.
- Fujii Y, et al. (2011) Colors of a Second Earth. II. Effects of Clouds on Photometric Characterization of Earth-like Exoplanets. *ApJ*738:184.
- Cowan NB, et al. (2011) Rotational Variability of Earth's Polar Regions: Implications for Detecting Snowball Planets. *ApJ*731:76.
- Cowan NB, Abbot DS, Voigt A (2012) A False Positive for Ocean Glint on Exoplanets: The Latitude-Albedo Effect. *ApJ*752:L3.
- Kaltenegger L, Traub WA, Jucks KW (2007) Spectral Evolution of an Earth-like Planet. *ApJ*658:598–616.
- Wordsworth R, Pierrehumbert R (2014) Abiotic oxygen-dominated atmospheres on terrestrial habitable zone planets. *ArXiv e-prints*.
- Seager S, Turner EL, Schafer J, Ford EB (2005) Vegetation's Red Edge: A Possible Spectroscopic Biosignature of Extraterrestrial Plants. *Astrobiology* 5:372–390.
- Montañes-Rodríguez P, Palle E, Goode PR, Martín-Torres FJ (2006) Vegetation Signature in the Observed Globally Integrated Spectrum of Earth Considering Simultaneous Cloud Data: Applications for Extrasolar Planets. *ApJ*651:544–552.
- Kiang NY, Siefert J, Govindjee, Blankenship RE (2007) Spectral Signatures of Photosynthesis. I. Review of Earth Organisms. *Astrobiology* 7:222–251.
- Baldrige AM, Hook SJ, Grove CI, Rivera G (2009) The ASTER spectral library version 2.0. *Remote Sensing of Environment* 113:711–715.
- McLinden CA, McConnell JC, Griffioen E, McElroy CT, Pfister L (1997) Estimating the wavelength-dependent ocean albedo under clear-sky conditions using NASA ER 2 spectroradiometer measurements. *Journal of Geophysical Research* 102:18801.
- Kokhanovsky A (2004) Optical properties of terrestrial clouds. *Earth Science Reviews* 64:189–241.
- Froehlich C, Shaw GE (1980) New determination of Rayleigh scattering in the terrestrial atmosphere. *Applied Optics* 19:1773–1775.
- Salomonson VV, Barnes WL, Maymon PW, Montgomery HE, Ostrow H (1989) MODIS - Advanced facility instrument for studies of the earth as a system. *IEEE Transactions on Geoscience and Remote Sensing* 27:145–153.